Biochimica et Biophysica Acta 1840 (2014) 2004–2013

Contents lists available at ScienceDirect

Biochimica et Biophysica Acta

journal homepage: www.elsevier.com/locate/bbagen

Curcusone D, a novel ubiquitin–proteasome pathway inhibitor via ROS-induced DUB inhibition, is synergistic with bortezomib against multiple myeloma cell growth

Mei-Na Cao [a], Yu-Bo Zhou [a,*], An-Hui Gao [a], Jia-Yi Cao [a], Li-Xin Gao [a], Li Sheng [a], Lei Xu [a], Ming-Bo Su [a], Xian-Chao Cao [a], Meng-meng Han [a], Ming-Kui Wang [b], Jia Li [a,*]

[a] National Center for Drug Screening, State Key Laboratory of Drug Research, Shanghai Institute of Materia Medica, Chinese Academy of Sciences, Shanghai 201203, China
[b] Chengdu Institute of Biology, Chinese Academy of Sciences, Chengdu 610041, China

ARTICLE INFO

Article history:
Received 15 June 2013
Received in revised form 24 January 2014
Accepted 4 February 2014
Available online 15 February 2014

Keywords:
Ubiquitin–proteasome pathway
Deubiquitinase
ROS
Curcusone D
Bortezomib
Multiple myeloma

ABSTRACT

Background: Ubiquitin–proteasome pathway (UPP) plays a very important role in the degradation of proteins. Finding novel UPP inhibitors is a promising strategy for treating multiple myeloma (MM).
Methods: Ub-YFP reporter assays were used as cellular UPP models. MM cell growth, apoptosis and overall death were evaluated with the MTS assay, Annexin V/PI dual-staining flow cytometry, poly (ADP-ribose) polymerase (PARP) cleavage, and PI uptake, respectively. The mechanism of UPP inhibition was analyzed by western blotting for ubiquitin, in vitro and cellular proteasomal and deubiquitinases (DUBs) activity assays. Cellular reactive oxygen species (ROS) were measured with H_2DCFDA.
Results: Curcusone D, identified as a novel UPP inhibitor, causes cell growth inhibition and apoptosis in MM cells. Curcusone D induced the accumulation of poly-ubiquitin-conjugated proteins but could not inhibit proteasomal activity in vitro or in cells. Interestingly, the mono-ubiquitin level and the total cellular DUB activity were significantly downregulated following curcusone D treatment. Furthermore, curcusone D could induce ROS, which were closely correlated with DUB inhibition that could be nearly completely reversed by NAC. Finally, curcusone D and the proteasomal inhibitor bortezomib showed a strong synergistic effect against MM cells.
Conclusions: Curcusone D is novel UPP inhibitor that acts via the ROS-induced inhibition of DUBs to produce strong growth inhibition and apoptosis of MM cells and synergize with bortezomib.
General significance: The anti-MM molecular mechanism study of curcusone D will promote combination therapies with different UPP inhibitors against MM and further support the concept of oxidative stress regulating the activity of DUBs.

1. Introduction

The ubiquitin–proteasome pathway (UPP) plays a vital role in the degradation of proteins involved in several pathways, including cellular proliferation and apoptosis. The proteasome is a validated target for multiple myeloma (MM) treatment; proteasomal inhibitors form a cornerstone of anti-myeloma therapy [1]. These inhibitors include bortezomib (PS-341), the first anti-MM proteasomal inhibitor that was FDA-approved, in 2003. Carfilzomib (Kyprolis), an epoxyketone with specific chymotrypsin-like activity, acts as an irreversible proteasomal inhibitor and was approved by the FDA in 2012 due to the improved response observed in relapsed and refractory MM patients previously treated with bortezomib [2]. However, in spite of its improved efficacy compared to alternative therapies, approximately 60% of patients do not respond to bortezomib due to the emergence of resistance.

In addition to proteasome, the UPP also includes ubiquitin, ubiquitin-activating enzymes (E1s), ubiquitin-conjugating enzymes (E2s), ubiquitin ligases (E3s) and deubiquitinases (DUBs), which collectively work in three discrete and successive steps: 1) the substrate is tagged by the covalent attachment of multiple ubiquitin molecules via E1, E2, and E3, 2) the tagged protein is degraded by the 26S proteasomal complex, and 3) poly-ubiquitins are recycled by DUBs to free ubiquitin for reuse [3]. Multiple myeloma is the most sensitive and the most responsive disease to proteasomal inhibitors, which implies that the UPP is critical for multiple myeloma pathophysiology. E1 [4], E2s such as CDC34 [5], E3s such as Mdm-2 [6] and SCF [7], and DUBs such as USP9X [8] are overexpressed and involved in multiple myeloma pathology. Furthermore, targeting such UPP components could sensitize MM cells susceptible to bortezomib-induced cell death [4,7]. Thus, targeting the entire UPP as opposed to proteasome alone is a promising strategy for multiple myeloma treatment.

* Corresponding authors at: 189 Guo Shou Jing Road, Shanghai 201203, China.
E-mail addresses: ybzhou@mail.shcnc.ac.cn (Y.-B. Zhou), jli@mail.shcnc.ac.cn (J. Li).

http://dx.doi.org/10.1016/j.bbagen.2014.02.006
0304-4165/

It has been shown that the functional analysis of the UPP can be accomplished by following the steady-state levels of GFP reporter substrates, which are typically based on an intrinsic fluorescent protein with a constitutively active degradation signal that targets the proteins for ubiquitination and proteasomal degradation [9]. Such a reporter system could be used to find new UPP inhibitors with distinct mechanisms and novel structures [10].

Here, the natural compound curcusone D, a diterpene isolated from *Jatropha curcas* (Barbados nut), an herbal plant that has been used in traditional folk medicine in many tropical countries, was identified to be a novel UPP inhibitor with the Ub-G76V-YFP reporter assay. The purpose of the present study was to investigate the mechanism of UPP inhibition by curcusone D and to further characterize its anti-MM effects. Curcusone D could not inhibit the proteasome's chymotrypsin-like, trypsin-like or caspase-like activities in vitro or at the cellular level, but it did inhibit the activity of DUBs in cells. Further mechanistic studies showed that curcusone D could induce ROS, which are responsible for the inhibition of DUBs and the UPP to induce cellular growth inhibition and apoptosis. Curcusone D could inhibit multiple myeloma cell growth and induce cellular apoptosis. The combination of curcusone D with bortezomib had significant synergistic effects on MM cell growth inhibition, apoptosis and UPP inhibition.

2. Materials and methods

2.1. Reagents and cell cultures

Ubiquitin Rhodamine-110 (Ub-R110) was purchased from Boston Biochem (Cambridge, MA, USA). 3-(4, 5-dimethylthiazol-2-yl)-5-(3-carboxymethoxyphenyl)-2-(4-sulfophenyl)-2H-tetrazolium (MTS) was purchased from Promega (Madison, WI, USA). The 2′,7′-dichlorofluoresceindiacetate (H_2DCFDA) fluorescent probe was obtained from Invitrogen (Grand Island, NY, USA). N-acetylcysteine (NAC) and trolox were purchased from Sigma-Aldrich (St. Louis, MO, USA). Bortezomib was generously provided from the East China Biotech Company (Shanghai, China). Curcusone D was kindly provided by Dr. Mingkui Wang (Chengdu Institute of Biology, Chinese Academy of Sciences, China) and dissolved in dimethyl sulfoxide (DMSO) to prepare a stock solution. The DMSO concentration was maintained between 0.1% and 1% in all cell cultures, which caused little detectable effect on cell growth or death.

Human multiple myeloma (MM) cell lines NCI-H929, RPMI 8226, SKO, KM-3, and LP-1 were gifted from Professor Jian Hou (Chang Zheng Hospital, Shanghai, China) and were grown in RPMI-1640 supplemented with 10% fetal bovine serum (FBS) and penicillin-streptomycin (Invitrogen, Grand Island, NY, USA) at 37 °C in a 5% CO_2 humidified atmosphere. To inhibit intracellular ROS generation, cells were pre-incubated with 10 mM NAC for 30 min prior to curcusone D treatment.

2.2. H1299-Ub-G76V-YFP, H1299-CD3δ-YFP, H1299-Ub-R-YFP, and H1299-YFP-CL1 cells

H1299 cells were maintained in RPMI-1640 medium, transfected with Ub-R-YFP, Ub-G76V-YFP, YFP-CL1, or CD3δ-YFP plasmids [11] (Addgene plasmids 11948, 11949, 11950, 11951) using Lipofectamine 2000 (Invitrogen, Grand Island, NY, USA), and selected with 800 μg/ml G418 (AMRESCO, Solon, OH, USA).

2.3. MTS assay

In a volume of 100 μL, human myeloma cells were seeded in 96-well plates at a density of 5×10^3 cells per well. After treatment with curcusone D for the indicated time, cells were incubated with MTS at a final concentration of 0.5 mg/ml for 2 to 4 h. Optical density was determined at 490 nm (background subtraction at 690 nm) with a SpectraMax 340 microplate reader (Molecular Devices, Sunnyvale, CA, USA). The growth inhibitory ratio was calculated as follows: growth inhibitory ratio $= (A_{control} - A_{sample})/A_{control}$. IC_{50} values were derived from a nonlinear regression model (curvefit) based on a sigmoidal dose response curve (variable slope) and computed using GraphPad Prism version 5.02, GraphPad Software. The drug combination index (CI) values were calculated with the software Calcusyn (version 2) (BioSoft, Milltown, NJ, USA) according to the manufacturer's instructions.

2.4. Antibodies and immunoblotting analysis

Poly ADP-ribose polymerase (PARP), ubiquitin, and GAPDH antibodies were purchased from Cell Signaling Technology (Boston, MA, USA); the β-actin antibody was obtained from Sigma, and the HA antibody was from Abmart (Shanghai, China). All antibodies were used as recommended by the manufacturers.

Whole-cell extracts were prepared in 1X sodium dodecyl sulfate (SDS) loading buffer, subjected to electrophoresis through 12% SDS-PAGE gels, and blotted with the indicated antibodies. The quantification of blot intensity was performed using *SmartView* software of the FR-980A Gel Image Analysis System (Shanghai Furi Science and Technology Co., Ltd., Shanghai, China). PARP cleavage is reported as the ratio of cleaved PARP to total PARP and expressed as a percentage. Ubiquitin is quantified as the ratio of the drug treatment group to the DMSO control group. HA Western blot densitometry graphics have been divided into 2 parts: the first includes downregulated proteins, which are mostly USPs, the other includes insignificantly changed proteins, which are UCHs as shown in Fig. 4.

2.5. Analysis of apoptosis using FCM of AV/PI dual staining

In this study, Annexin V-FITC (fluorescein isothiocyanate)/PI (propidium iodide) staining for FCM was used to detect apoptosis quantitatively and qualitatively. Cells were processed with an Annexin V-FITC kit (Keygene, Nanjing, China) following treatment according to the manufacturer's instructions. Next, the samples were analyzed using the FACScan flow cytometer (Becton Dickinson, Sparks, MD, USA) to quantify the apoptotic rate. Different subpopulations were distinguished using the following criteria: Q1, Annexin V-negative, but PI-positive (i.e., necrotic cells); Q2, Annexin V/PI-double positive (i.e., late apoptotic cells); Q3, Annexin V/PI-double negative (i.e., live cells); Q4, Annexin V-positive, but PI-negative (i.e., early apoptotic cells). The apoptotic rate was determined as the percentage of Q2 + Q4.

2.6. PI uptake assay

Cells were washed twice with PBS. After centrifuging at 1000 ×*g* for 5 min at 4 °C, the supernatants were collected and resuspended in 500 μl of PBS containing 10 μg/ml propidium iodide (PI) and 40 μg/ml RNase. Next, the samples were analyzed using the FACScan flow cytometer to quantify the cell death rate.

2.7. Measurement of intracellular ROS generation

After treatment with curcusone D, cells were harvested and washed with phosphate-buffered saline (PBS) and then resuspended in 1 ml of PBS. Cells were incubated with 10 μM H_2DCFDA in the dark at 37 °C for 15 min. Cells were then washed and collected in PBS and measured by FACS flow cytometry (Becton Dickinson, Sparks, MD, USA) with 485 nm excitation and 525 nm emission.

2.8. Purified proteasomal activity assay

A quantity of 1 μl of test compound was added to 10 μl purified human proteasomes (60 μg/ml for VR3, 25 μg/ml for LE3 and 5 μg/ml

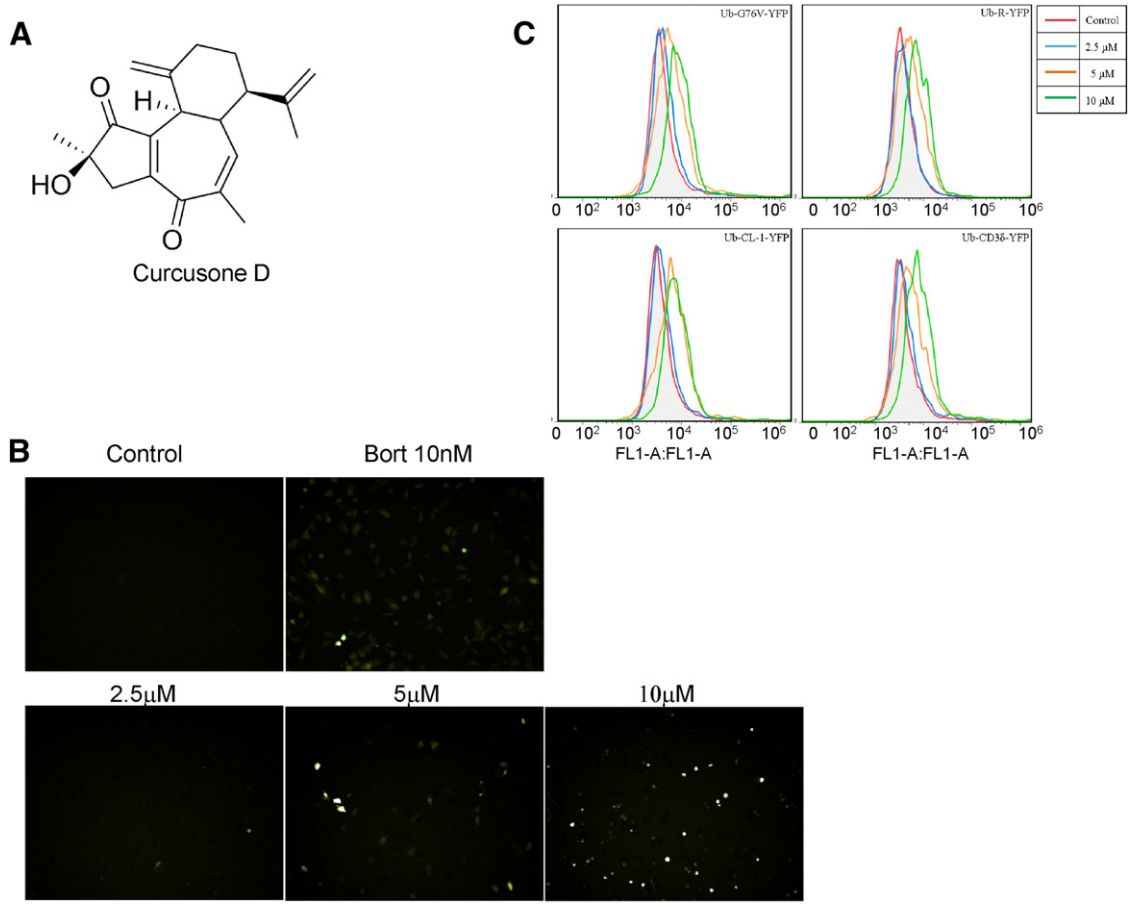

Fig. 1. Curcusone D induced UPP inhibition in cells. (A) Chemical structure of curcusone D. (B) H1299-Ub-G76V-YFP cells were treated with curcusone D for 24 h, and the YFP fluorescence was analyzed with the Operetta analysis system (PerkinElmer, Waltham, MA, USA). Fluorescence in untreated cells, positive control proteasomal inhibitor bortezomib-treated cells (10 nM), and curcusone D-treated cells at 2.5, 5 and 10 μM was shown. (C) H1299 Ub-CL1-YFP, Ub-CD3δ-YFP, Ub-G76V-YFP, and Ub-R-YFP cells were treated with curcusone D for 24 h; samples were collected, and YFP intensity was detected with flow cytometry.

for LY4), a gift from Dr. Jiang-ping Wu (Notre-Dame Hospital, Montreal, Quebec, Canada), incubated for 15 min, and then supplemented with 39 μl synthesized substrate (GL Biochem Ltd., Shanghai, P.R. China), 37.5 μM Bz-Val-Gly-Arg-AMC (VR3, trypsin-like), 37.5 μM Z-Leu-Leu-Glu-AMC (LE3, caspase-like), and 37.5 μM Suc-Leu-Leu-Val-Tyr-AMC (LY4, chymotrypsin-like) synthesized substrates (GL Biochem Ltd., Shanghai, P.R. China). The AMC probe was detected by monitoring the increase of fluorescence with Envision at 355 nm excitation and 460 nm emission.

2.9. Cellular proteasomal activity assay

Cells were washed twice with PBS, and cell fractionation was performed as described [12]. In brief, after washing the cells with PBS, the pellet was suspended in 300 μl ice cold buffer A (20 mM HEPES pH 7.5, 1.5 mM $MgCl_2$, 10 mM KCl, 1 mM EDTA, 1 mM EGTA, 1 mM DTT and 0.1 mM phenylmethylsulfonyl fluoride (PMSF) with 10 mg/ml each of aprotinin, pepstatin and leupeptin containing 250 nM sucrose). The cells were then homogenized for three minutes in a Dounce homogenizer with a sandpaper-polished pestle. A total of 10 μg of lysate was added to 11 μl substrate buffer (20 mM HEPES (pH 8.2), 0.5 mM EDTA, 1% DMSO, 1 mM ATP), and the mixture was incubated for 15 min and supplemented with 39 μl substrate, 60 μM Bz-Val-Gly-Arg-AMC (trypsin-like), 60 μM Z-Leu-Leu-Glu-AMC (caspase-like), and 60 μM Suc-Leu-Leu-Val-Tyr-AMC (chymotrypsin-like) probes. The AMC probes were detected by monitoring the increase of fluorescence with Envision at 355 nm excitation and 460 nm emission.

2.10. Cellular assay for DUBs

A total of 15 μg of cells were subjected to a RIPA lysis buffer (Thermo Fisher Scientific Inc. Rockford, IL, USA) and added individually to 20 μl deubiquitination assay buffer (50 mM Tris–HCl (pH 7.4), 20 mM potassium chloride, 5 mM magnesium chloride, 0.75 μM Ub-R110). The fluorescence intensity was immediately measured using a PE Envision luminescence spectrometer with excitation and emission wavelengths set at 485 and 535 nm, as previously indicated [13].

2.11. DUB active site probe assay

Cells were lysed for 1 h in ice-cold RIPA lysis buffer (Thermo Fisher Scientific Inc. Rockford, IL, USA). The supernatants from cell lysates were collected after 10 min of centrifugation at 14,000 rpm at 4 °C. A total of 30 μg of lysate was incubated with 0.3 μg of HA-Ub-VS probe (Boston Biochem, Cambridge, MA, USA) in a total volume of 30 μl of homogenization buffer (50 mM Tris (pH 7.5), 5 mM $MgCl_2$, 0.5 mM EDTA, 2 mM ATP and 250 mM sucrose) at 37 °C for 30 min, then boiled for 10 min and processed for anti-HA Western blot analysis.

2.12. Statistical analysis

All data are presented as the mean ± standard deviation (SD). Statistical significance was determined using Student's *t*-test. *, **, and *** indicate *t*-test P values of < 0.05, 0.01, and 0.001, respectively.

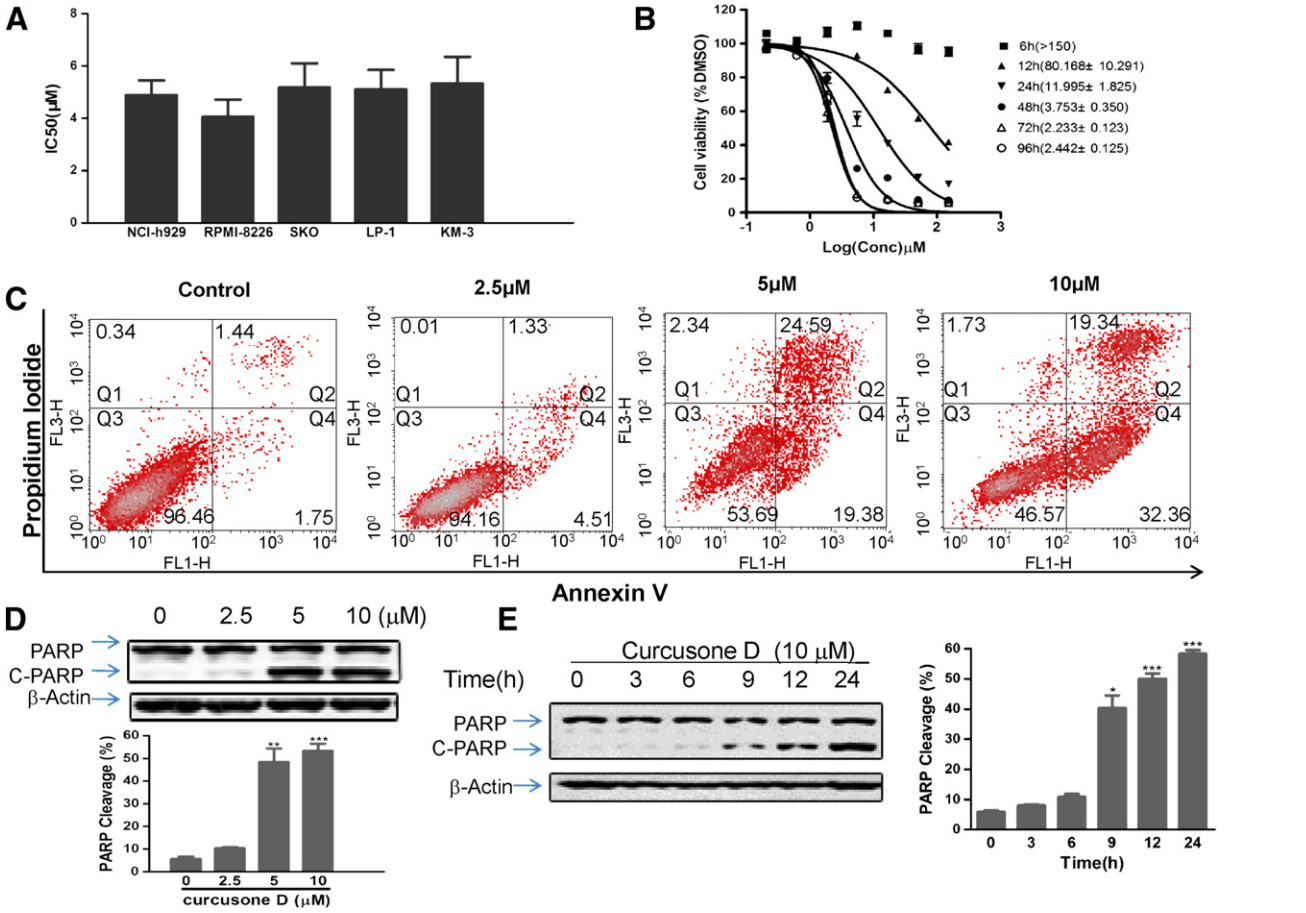

Fig. 2. Assessment of the proliferation inhibition and cellular apoptosis induced by curcusone D in MM cells. (A) The cell growth inhibition of MM cells by curcusone D was evaluated in NCI-H929, RPMI 8226, SKO, LP-1, and KM-3 MM cell lines by the MTS assay. (B) NCI-H929 cells were treated in the indicated 6, 12, 24, 48, 72, and 96 h with curcusone D at six doses. And the IC_{50} at the related time point was calculated. (C) The percentage of apoptotic cells was analyzed by flow cytometry for Annexin V/propidium iodine (PI) double staining. Whole-cell extracts were detected with cleaved PARP as an indicator for the onset of apoptosis. H929 cells were treated with various concentrations (2.5, 5 or 10 μM) of curcusone D for 24 h (D) or curcusone D at 10 μM for 0 to 24 h (E) before their extracts were probed for the presence of PARP proteins. β-Actin was probed on the same blot as a protein loading control.

3. Results

3.1. Curcusone D inhibits UPP

To discover novel inhibitors of the UPP, a cellular reporter assay for proteasomal activity was established. Human H1299 lung cancer cells were engineered to express a Ub-G76V-YFP reporter protein [11] to create H1299-Ub-G76V-YFP cells. Following treatment with the positive control proteasomal inhibitor bortezomib, Ub-G76V-YFP fluorescence increased in H1299-Ub-G76V-YFP cells compared to the untreated control cells (Fig. 1B). Curcusone D (Fig. 1A) also increased YFP fluorescence in H1299-Ub-G76V-YFP cells in a dose-dependent manner (Fig. 1B), indicating that the UPP was suppressed. Different UPP substrates can be regulated by different E1s, E2s, and E3s. To evaluate the substrate specification of curcusone D, other three YFP-based reporters were tested by FACS. These reporters represent different classes of UPP substrates, including the ERAD substrate, CD3δ-YFP, the N-end rule substrate, Ub-R-YFP, and the misfolded degradation substrate, YFP-CL1. Curcusone D also increased the YFP intensity of these other three substrates in a dose-dependent manner (Fig. 1C), implying that the targets for curcusone D are not in a selective portion of the UPP.

3.2. Curcusone D inhibits MM cell growth and induces cellular apoptosis

To test the effect of curcusne D on cell growth, five MM cell lines was evaluated by the MTS assay (Fig. 2A). After 48 h of treatment, curcusone D displayed potent anti-proliferative effects against NCI-H929, RPMI 8226, SKO, LP-1 and KM-3 cells with IC_{50}s of 4.889 ± 0.563, 4.064 ± 0.654, 5.188 ± 0.920, 5.111 ± 0.745, and 5.332 ± 2.522 μM, respectively. Furthermore, curcusone D inhibited MM cell growth in a time-dependent manner: the IC_{50} of curcusone D in NCI-H929 cells dropped significantly as treatment time increased (Fig. 2B). NCI-H929 cells were used in the following mechanistic and anti-cancer studies.

To evaluate apoptosis induced by curcusne D, the FACS analysis of Annexin V-FITC/PI dual staining was performed in NCI-H929 cells treated with 2.5, 5, and 10 μM of curcusone D for 24 h. As shown in Fig. 2C, curcusone D could induce a significant dose-dependent increase in the apoptotic rate [(Q2 + Q4) %]. Moreover, after 24 h of treatment, cleaved poly ADP-ribose polymerase (PARP) increased in a dose- and time-dependent manner (Fig. 2D and E).

3.3. Curcusone D could not inhibit proteasomal activity

Ubiquitination is a covalent post-translational modification of cellular proteins involving a complex enzymatic cascade, which reflects the UPP status [14]. As previously demonstrated [15] (Fig. 3A and B), curcusone D inhibit the UPP status is consistent with the positive control bortezomib. Western blotting showed that in curcusone D-treated NCI-H929 cells, the ubiquitined protein accumulation in a marked time- and concentration-dependent manner. However, whether curcuone D inhibits proteasomal activity is unclear. So, next, we assessed the effects of curcusone D on purified proteasomal activity. As Supplemental Fig. 1 shown, the positive proteasome inhibitor control, bortezomib substantially inhibited proteasomal activity as others have reported.

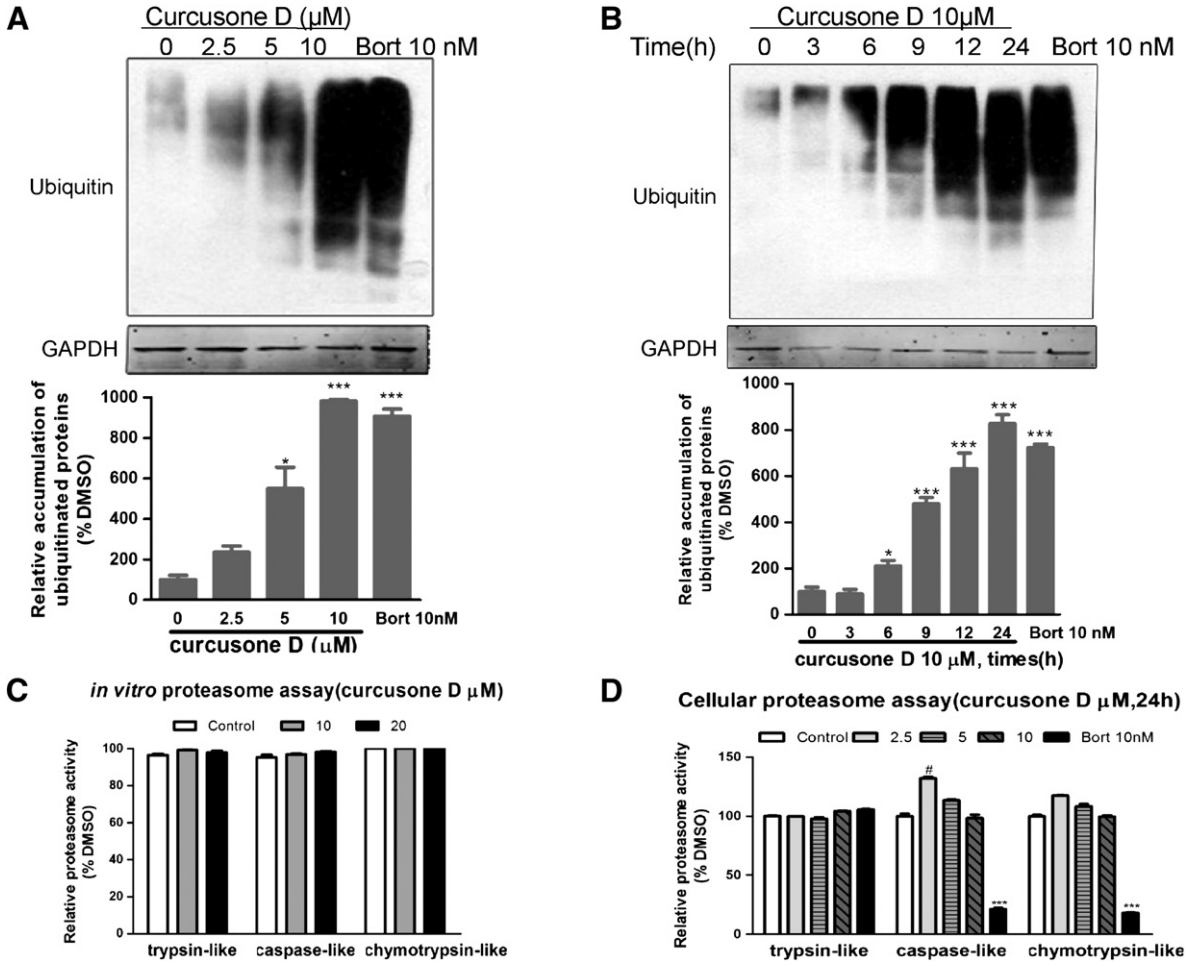

Fig. 3. Curcusone D did not inhibit proteasomal activity in vitro or in cells. H929 cells were treated with various concentrations (2.5, 5 or 10 μM) of curcusone D for 24 h (A) or curcusone D at 10 μM for 0 to 24 h (B). Poly-ubiquitinated proteins were determined by western blotting; sample from cells treated with 10 nM of bortezomib was used as a positive control. (C) Purified proteasomes were incubated with 10 or 20 μM of curcusone D, for 15 min, and the proteasome chymotrpsin-like, caspase-like, and trpsin-like protease activities were detected with the above indicated methods. (D) H929 cells were treated with curcusone D for 24 h and harvested. Cytosolic extracts were then analyzed for chymotryptic-like, tryptic-like and caspase-like proteasomal activities. The results are presented as the percentage inhibition of proteasomal activities in drug treatments versus vehicle control treatments.

However, treatments with curcusone D at 2.5, 5, or 10 μM for 2 h caused no significant decline in purified proteasomal chymotrypsin-like, trypsin-like or caspase-like activities (Fig. 3C), which implied that curcusone D could not directly inhibit the proteasome in vitro. The effects of curcusone D on cellular proteasomal activity were then assessed in H929 cells (Fig. 3D). In parallel, curcusone D treatments at 2.5, 5, and 10 μM for 24 h were also unable to inhibit the cellular proteasomal chymotrypsin-like, trypsin-like or caspase-like activities. However, slight increased of chymotrypsin- and caspase-like activities were observed with the 2.5 μM treatment. The reference compound bortezomib still exerted strong proteasomal inhibition activity. The in vitro and cellular results suggested that unlike bortezomib, curcusone D does not block proteasomal activity.

3.4. Curcusone D inhibits DUB activity in cells with partial selectivity

As Fig. 3 shown, curcusone D neither affects the attachment of multiple ubiquitins to substrates nor inhibit proteasome activity. So, the DUB activity was tested, since the inhibition of cellular DUBs could also lead to an increase in high-molecular weight ubiquitinated proteins in the absence of proteasomal inhibition (23, 41). A rapid depletion of monomeric ubiquitin was detected in curcusone D-treated cells (Fig. 4A). This observation suggests that curcusone D may reduce ubiquitin recycling and cause a buildup of ubiquitinated proteins through the inhibition of DUB activity. Thus, it was prudent to measure the effect of curcusone D on the activity of DUBs. The ubiquitin-fused fluorogenic substrate for DUBs based on the C-terminal derivative of ubiquitin with rhodamine 110 (R110) was used to evaluate the total cellular DUB activity as previously described [13]. H929 cells were treated with curcusone D at 2.5, 5 and 10 μM for 6 or 24 h and analyzed for the total cellular DUB activity. As Fig. 4B shown, curcusone D significantly inhibited the total cellular DUB activity in a dose- and time-dependent manner.

There are nearly 100 DUBs in the human genome. To clarify the inhibition of DUB activity by curcusone D, cell lysates from control and treated cells were incubated with HA-Ub-VS, which acts as a DUB suicide substrate by forming a covalent adduct with active DUB enzymes. Specific cellular DUBs can be identified by anti-HA blotting, as previously shown in various cell types [16–18]. Changes in specific DUB activities are measurable by monitoring the HA label in lysates from control and treated cells, as previously mentioned. A marked reduction in the labeling of the DUBs USP5, USP7, USP8, USP15, USP14 and USP22 was observed in cells treated with curcusone D at 10 μM for 24 h. An insignificant change in the labelings of UCH-37, UCH-L1 and UCH-L3 were noted, implying that curcusone D induced partially selective DUB inhibition (Fig. 4C).

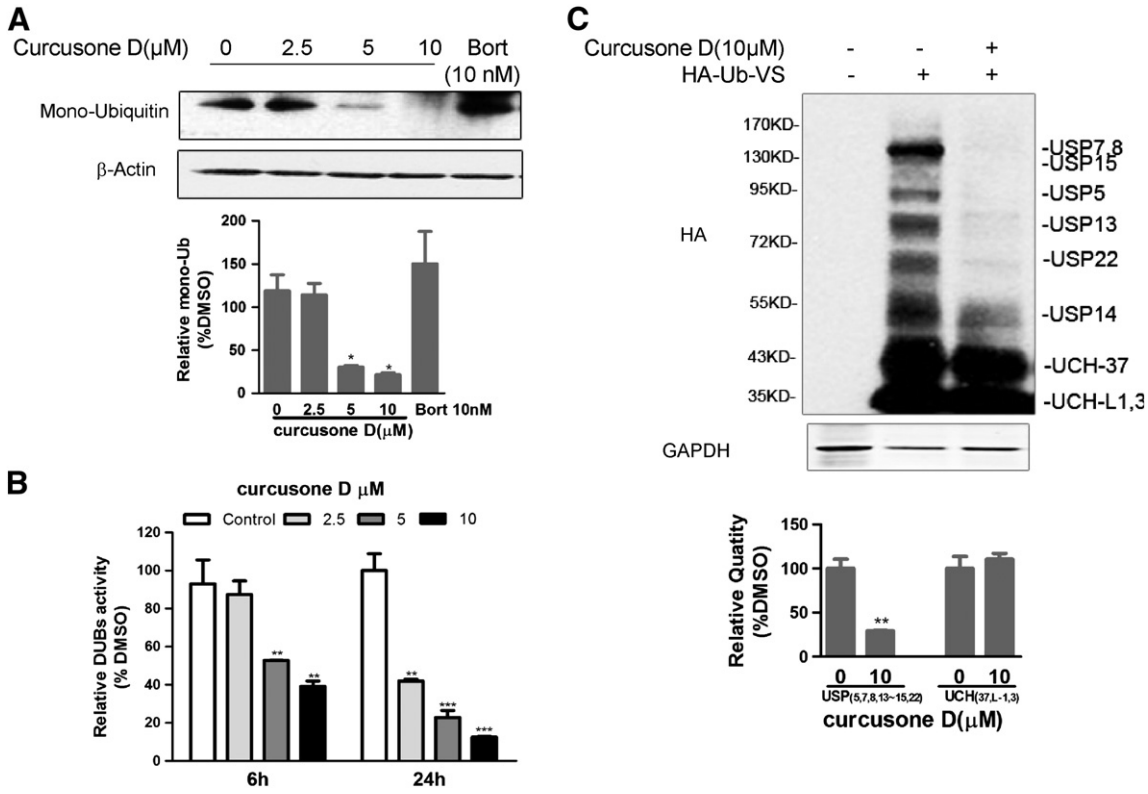

Fig. 4. Curcusone D inhibited the activity of DUBs with partial selectivity in cells. (A) H929 cells were treated with 2.5, 5, or 10 μM of curcusone D for 24 h. Mono-ubiquitin was detected by western blotting; the positive control is sample from cells treated with 10 nM of bortezomib. (B) The effect of curcusone D on the activity of DUBs was detected with ubiquitin-R110. H929 cells were treated with curcusone D at 2.5, 5, and 10 μM for 6 and 24 h and analyzed for the total DUB activities. (C) H929 cells were lysed in DUB labeling buffer as described in the Materials and methods section. The clarified supernatant (30 μg) was incubated with 0.3 μg HA-Ub-VS for 30 min at 37 °C. HA immunoblotting was used to assess the changes in DUB labeling.

3.5. Curcusone D induces ROS, which are required for the inhibition of DUBs and cell growth

Curcusone D shares no structural or chemical resemblance to any known DUB inhibitors [19–24] despite its ability to inhibit the activities of many cellular DUBs (Fig. 4C), establishing it as a new, partially selective DUB inhibitor. We tried to find the new mechanism of selective DUB inhibition. It is reported that many DUBs, such as the E1, E2, and E3 enzymes, contain active site cysteine residues that are prone to oxidation, which inactivates the enzyme [25]. To check whether the DUBs were inhibited by curcusone D via oxidative stress, the ROS burst in cells treated with curcusone D was tested. The cell-permeable H_2DCFDA probe was used as a fluorescent indicator of the changes in ROS levels in cells. As Fig. 5A shown, curcusone D treatment for 3 h induced ROS production in a dose-dependent manner. The ROS scavenger N-acetyl cysteine (NAC) blocked curcusone D-induced ROS production (Fig. 5B). The potential for NAC to rescue DUB and UPP inhibition by curcusone D was tested. The activities of DUBs were evaluated with Ub-R110. As Fig. 5C shown, NAC could nearly reverse the inhibition of DUBs by curcusone D, which indicated that ROS production is required for the inhibition of DUBs. Interestingly, the UPP inhibition was also reversed by NAC; the accumulation of poly-ubiquitinated proteins induced by curcusone D was limited (Fig. 5D). Furthermore, NAC could also block the curcusone D-induced cell growth inhibition and apoptosis, as determined by morphology observation and PARP cleavage, respectively (Fig. 5E and F).

3.6. Curcusone D in combination with bortezomib synergistically enhances cell growth inhibition and apoptosis in H929 cells

Considering the different targets in the UPP pathway between curcusone D and bortezomib, the synergistic effect of curcusone D in combination with bortezomib against myeloma cells was assessed. As Fig. 6A shown, 2.5 μM of curcusone D in combination with 2.5, 5 or 10 nM of bortezomib significantly enhanced cell growth inhibition after 48 hour treatments in H929 cells. Moreover, statistical analysis indicated that a high degree of synergy were present between bortezomib and curcusone D at all concentrations tested in H929 cells, as the drug combination index (CI) values calculated with the software Calcusyn were less than 1 (Table 1).

The PI uptake assay was used to further evaluate the synergistic effect on myeloma H929 cells. As Fig. 6B shown, after treating H929 cells with curcusone D alone or in combination with bortezomib for 24 h, cells were harvested and analyzed by FACS for PI uptake. There are noticeably more PI-positive cells after the combination treatment compared to either of the compounds alone, further indicating synergy between curcusone D and bortezomib (Fig. 6B). Accordingly, PARP cleavage, a reliable apoptosis indicator that is detected by western blotting, also showed enhanced apoptosis in the combination treatment group (Fig. 6C). The analysis of whole-cell extracts from curcusone D-treated NCI-H929 cells by western blotting for ubiquitin showed a marked concentration-dependent accumulation of ubiquitinated proteins in the combination treatment (Fig. 6D), indicating that curcusone D in combination with bortezomib synergistically enhances the inhibition of the UPP in MM cells.

4. Discussion

UPP components including the proteasome, E1s, E2s, E3s and DUBs may become one the most important classes of therapeutic targets for the pharmaceutical industry in the near future and supersede those which are involved in the phosphorylation system [26]. Until recently, there have been no UPP component regulators approved by the FDA except proteasomal inhibitors. An E1 inhibitor and inhibitors of E3 are

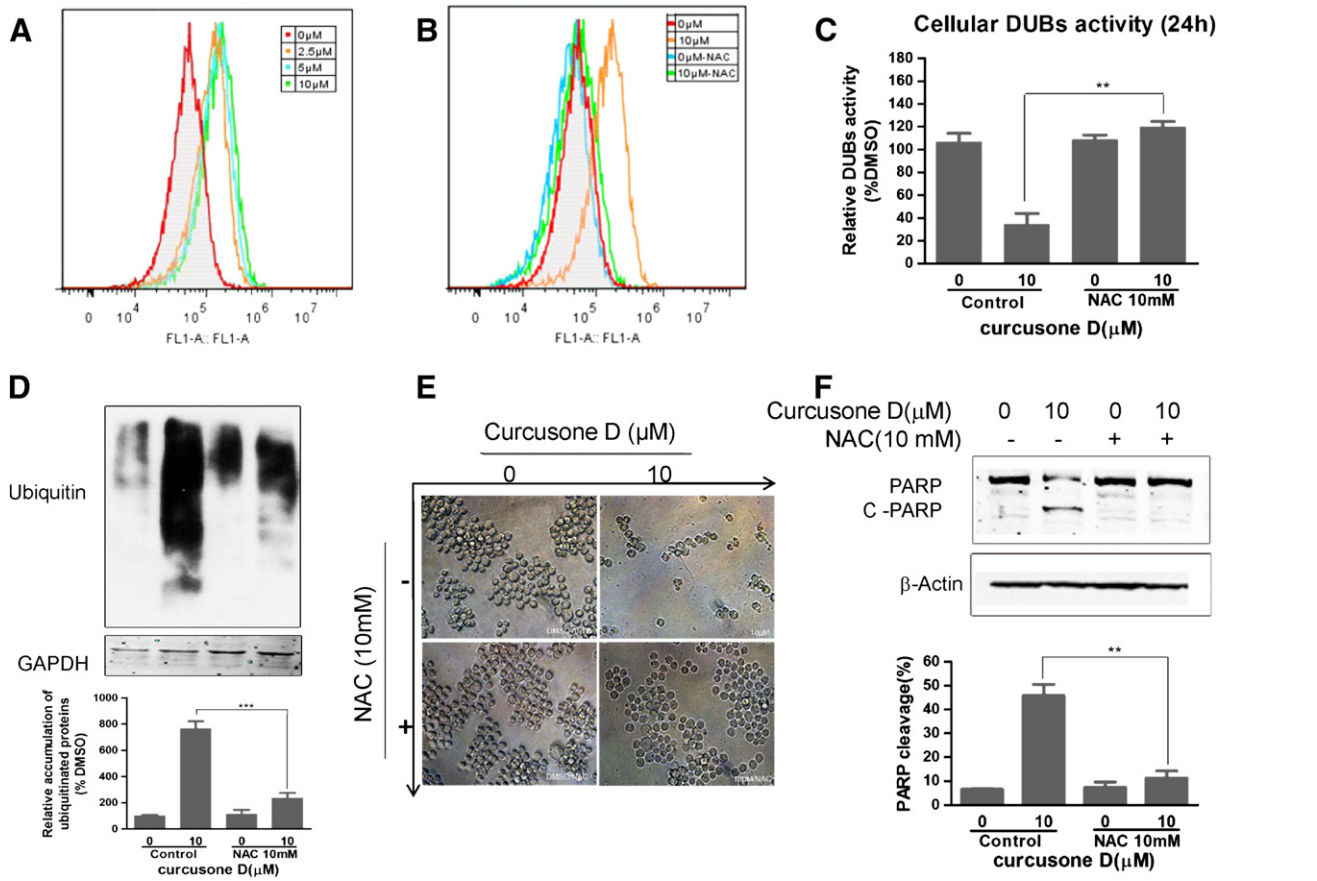

Fig. 5. ROS generation is responsible for curcusone D-induced DUB inhibition and cell growth inhibition. (A) H929 cells were treated with curcusone D at 2.5, 5 and 10 μM for 3 h and then incubated with the fluorescent probe H_2DCFDA for ROS detection. The redox cycling ability of curcusone D was detected by flow cytometry. (B) Cells were pre-incubated with 10 mM NAC and then treated with 10 μM of curcusone D for 3 h. The ROS level was determined using H_2DCFDA. (C) H929 cells were pretreated with 10 mM of NaCl or NAC for 30 min and then treated with 10 μM of curcusone D for 24 h and analyzed for the total DUB activities with Ub-R110. (D) Ubiquitinated proteins were determined by western blotting. (E) The cell growth inhibition by curcusone D alone or pre-incubated with NAC was observed by optical microscopy after 24 h. (F) The PARP cleavage in cells treated with curcusone D alone or pre-incubated with NAC was determined by western blotting. The densitometry graphics for 3 independent western blotting results are shown.

now in clinical trials, whereas no E2 or DUB inhibitors have entered clinical trials [19,27]. In recent years, some small-molecule DUB inhibitors have been identified possessing good selectivity against 19S RP-associated DUBs (USP14 and UCH-L5) such as b-AP15 [24], but most of the DUB inhibitors have poor selectivity. Additionally, the mechanisms of small chemical DUB inhibitors are elusive.

The chemical structure of curcusone D is different from all of the reported DUB inhibitors. It contains cross-conjugated α, β-unsaturated ketones (Fig. 1A). A similar pharmacophore was previously described in the pan-DUB inhibitor prostaglandin lipid derivatives, which function as potent Michael receptors to inhibit the activities of DUBs [28,29]. The alpha, beta-unsaturated carbonyl center in the cyclopentenone ring of prostaglandins could react with the DUB catalytic cysteine thiol group, resulting in a covalent adduct [30]. Our results indicated that curcusone D could induce ROS, which are responsible for the inhibition of DUBs (Fig. 5C), similar to the activity of prostaglandin.

However, it has been reported that NAC is not only an ROS scavenger but can also antagonize the activity of the proteasomal inhibitor piperlongumine via direct interaction [31]. Trolox, another ROS scavenger that could not interact with proteasomal inhibitors, was used to further evaluate whether Trolox could reverse curcusone D induced polyubiquitin level. As the Supplemental Fig. 2 showed, trolox also could significantly reverse the Curcusone D induced polyubiquitin level. So, here we showed that both NAC and Trolox could reverse the effect of Curcusone D on protein polyubiquitin, which indicated that Curcusone D might not like the proteasome inhibitor piperlongumine [31], which could only be reversed by NAC via a direct interaction with NAC. And as Supplemental Fig. 3 shown, trolox also significantly reversed the curcusone D-induced cell growth inhibition in a dose-dependent manner in both NCI-H929 and RPMI-8226 multiple myeloma cells, which confirmed that the inhibition of cell growth by curcusone D requires ROS production.

There are 100 putative DUBs encoded by the human genome, which consist of five different families, of which four are cysteine proteases (ubiquitin C-terminal hydrolase (UCH), ubiquitin specific protease (USP/UBP), ovarian tumor domain (OTU), and Josephin domain (MJD) subfamilies), and one contains a metalloprotease (the JAMM subfamily) [32,33]. Recently, it has been confirmed that not all but many DUBs including USP, UCH and OUT subfamily members could be reversibly inactivated by H_2O_2 treatment in vitro and in cells [33–35]. Curcusone D inhibited USP5, 7, 8, 13, 14, 15, and 22 activities, but had no effect on UCH-L1, UCH-L3, and UCH-37 (Fig. 4C), which indicates the different sensitivity of DUB members to ROS as mentioned previously [33–35]. Still, there are some differences between curcusone D and H_2O_2 treatment, such as that UCH-L1 and UCH-L3 could not be inhibited by curcusone D but could be actually inhibited by H_2O_2 [34,36]. Additionally, chalcone-based derivatives AM146, RA-9 and RA-14, which contain α,β-unsaturated carbonyl groups, directly target and suppress the activity of UCH-L1, UCH-L3, USP2, USP5 and USP8 without affecting the 20S proteasome catalytic-core activity [37]. More details of oxidative stress regulating DUBs could be uncovered as more and more small molecular probes, including curcusone D, are identified in the future. The oxidation of the sulfenic acid group (SOH) at the cysteine residue inhibits the activity of DUBs, which could be reversed in the presence of a reducing

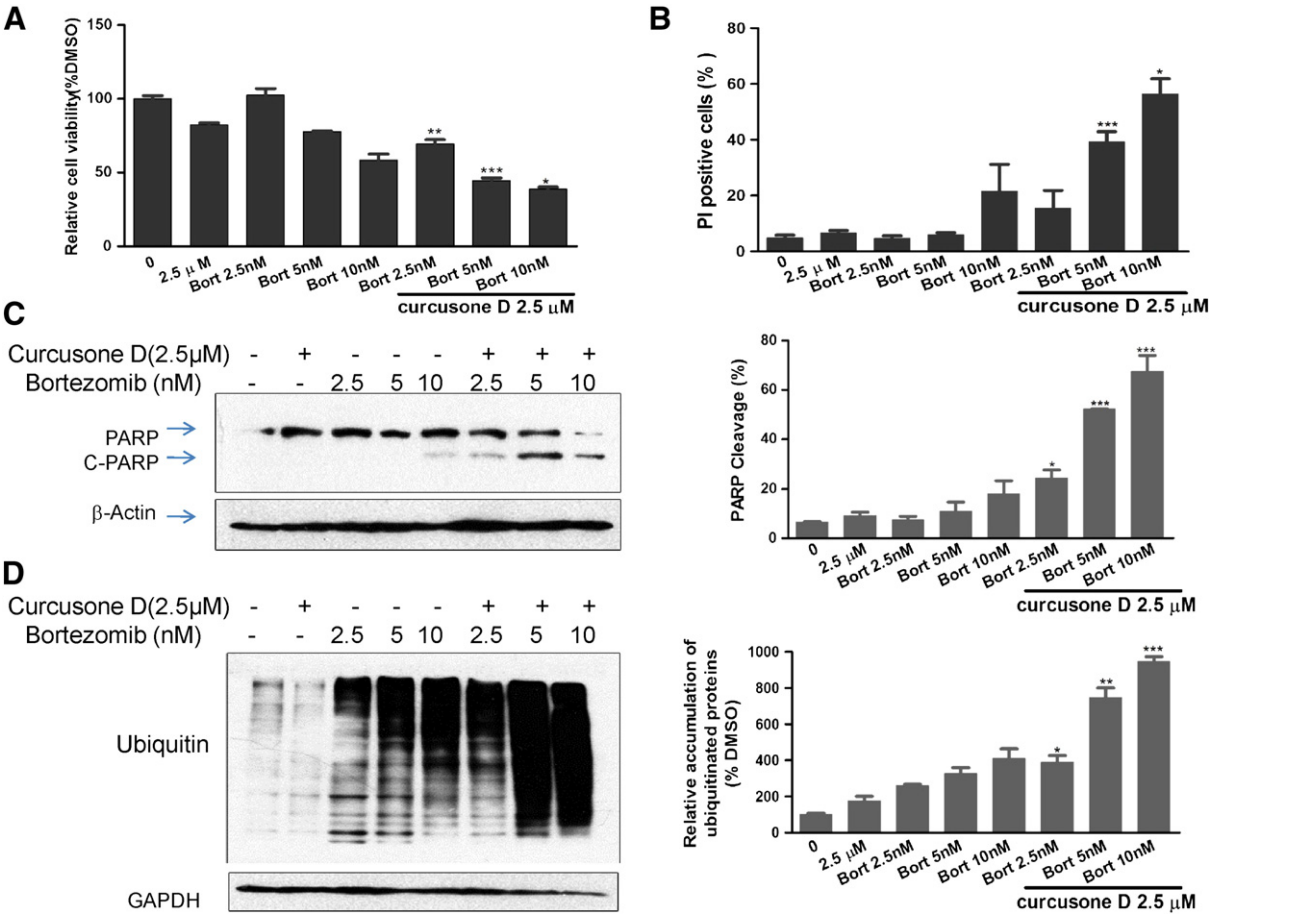

Fig. 6. Curcusone D in combination with bortezomib synergistically enhances cell growth inhibition and apoptosis in H929 cells. (A) H929 cells were treated with 2.5 μM of curcusone D with or without bortezomib (2.5, 5 and 10 nM) for 48 h, and the proliferation inhibitory ratio (%) was calculated by the MTS assay. (B) H929 cells were treated with curcusone D with or without bortezomib (2.5, 5 and 10 nM) for 24 h, and apoptotic cells were analyzed by flow cytometry of propidium iodine (PI) staining. PARP cleavage (C) and ubiquitination (D) were determined by western blotting. The densitometry graphics for 3 independent Western blotting results are shown.

agent, but further oxidation to sulfinic acid (SO_2H) or sulfonic acid (SO_3H) could induce the degradation of DUBs [38]. As Fig. 3C shown, the HA labeling of DUBs decreased significantly with curcusone D treatment, implying that the activity of some DUBs, including USP5, 7, 8, 13, 14, 15 and 22, was downregulated. However, whether the related DUB protein levels were downregulated deserves specific attention in future studies, which may indirectly reveal the oxidative status of these DUBs.

All components of the UPP were predicted to be susceptible to oxidative stress due to the cysteine residues in their active sites [36]. Curcusone D inhibits DUBs but has no significant effect on the action of E1, E2s, E3s, or the proteasome, which indicates that the targets of the ROS induced by curcusone D have some selectivity. That might be caused by the different sensitivity of proteins to ROS or the preferred binding of curcusone D to particular DUBs.

UPP inhibition could cause the accumulation of many proteins that regulate many different pathways involved in cellular apoptosis and cell proliferation. Proteasomal inhibitors could induce the TRAIL apoptotic pathway, activate the JNK pathway, and downregulate the expression of growth-signaling pathway components, including NFκB and the Akt/mTOR pathway [39–42]. The cytotoxicity induced by the USP7-selective inhibitor P5091 is mediated in part via the HDM2-p21 signaling axis and is independent of p53 [43]. WP1130, an inhibitor of USP9x, USP5, USP14, and UCH37, caused the downregulation of the pro-survival protein Mcl-1, induced aggresome formation, and facilitated apoptosis [44]. We have found that curcusone D could inhibit NFκB reporter luciferase expression and activate the JNK pathway (data not shown). The mechanism of the pathways that are regulated by curcusone D to produce its anti-cancer effects needs to be further elucidated.

Peripheral nerve damage is one of the most significant non-hematologic toxicities of bortezomib, which often leads to dose modification and potential changes in the patient's treatment plan when it occurs [45]. Other UPP component inhibitors, including a SCF^{Skp2} E3 inhibitor, act synergistically with bortezomib [7]. Here, we identified that curcusone D combined with bortezomib had synergistic effects on MM cell growth inhibition, cell apoptosis and total ubiquitinated proteins (Fig. 6), which could enhance the potential use of a DUB inhibitor combined with a proteasomal inhibitor. The DUB inhibitor P5091 could induce synergistic anti-MM activity with lenalidomide or Dex

Table 1
Combination indices of bortezomib and curcusone D in H929 cells.

Bortezomib (nM)	Curcusone D (μM)	CI
3	2.5	0.69
6	2.5	0.45
10	2.5	0.39
3	5.0	0.49
6	5.0	0.35
10	5.0	0.36
3	10.0	0.41
6	10.0	0.4
10	10.0	0.36

Combination indices are shown for H929 cells treated for 48 h with the indicated concentrations of bortezomib and curcusone D. Data were analyzed using Calcusyn (version 2) software (BioSoft, Milltown, NJ). The combination index (CI) is a quantitative measure of the degree of drug interaction, with a CI < 1 indicating synergy, a CI = 1 indicating additive effects, and a CI > 1 indicating antagonistic activity.

amethasone (Dex) [43]. In the future, curcusone D combination therapy to overcome bortezomib resistance or in combination with other clinical agents such as lenalidomide or Dex will be further evaluated.

It has been observed that Curcusone D has a strong inhibitory effect against lymphoma and cervical carcinoma cells [46]. Curcusone B, another diterpene isolated from *J. curcas*, could also effectively suppress cancer cell metastasis [47]. However, the anti-cancer effects and mechanism of curcusone D are still unclear. Here, we have reported for the first time that curcusone D could inhibit the UPP pathway via ROS-induced DUB inhibition, which in terms suppress myeloma cell growth. Curcusone D also induces apoptosis and acts synergistically with bortezomib, which may improve the anti-cancer use of the herbal plant *J. curcas*. Importantly, the pharmacokinetics and bioavailability of curcusone D and the effective anti-cancer dosages in mouse cancer model need to be evaluated in next stage.

Supplementary data to this article can be found online at http://dx.doi.org/10.1016/j.bbagen.2014.02.006.

Acknowledgements

This work was supported by grants from the National Natural Science Foundation of China (Nos. 91029716, 81072667, and 81125023) and the National Science and Technology Major Projects for "Major New Drugs Innovation and Development" (2012ZX09301001-004). We are grateful to Professor Jian Hou (Chang Zheng Hospital, Shanghai, China) for the presentation of NCI-H929, RPMI 8226, SKO, KM-3, and LP-1 human multiple myeloma (MM) cell lines.

References

[1] P. Moreau, P.G. Richardson, M. Cavo, R.Z. Orlowski, J.F. San Miguel, A. Palumbo, J.L. Harousseau, Proteasome inhibitors in multiple myeloma: 10 years later, Blood 120 (2012) 947–959.
[2] J.L. Thompson, Carfilzomib: a second-generation proteasome inhibitor for the treatment of relapsed and refractory multiple myeloma, Ann. Pharmacother. 47 (2013) 56–62.
[3] M.H. Glickman, A. Ciechanover, The ubiquitin–proteasome proteolytic pathway: destruction for the sake of construction, Physiol. Rev. 82 (2002) 373–428.
[4] G.W. Xu, M. Ali, T.E. Wood, D. Wong, N. Maclean, X. Wang, M. Gronda, M. Skrtic, X. Li, R. Hurren, X. Mao, M. Venkatesan, R. Beheshti Zavareh, T. Ketela, J.C. Reed, D. Rose, J. Moffat, R.A. Batey, S. Dhe-Paganon, A.D. Schimmer, The ubiquitin-activating enzyme E1 as a therapeutic target for the treatment of leukemia and multiple myeloma, Blood 115 (2010) 2251–2259.
[5] D. Chauhan, G. Li, T. Hideshima, K. Podar, R. Shringarpure, C. Mitsiades, N. Munshi, P.R. Yew, K.C. Anderson, Blockade of ubiquitin-conjugating enzyme CDC34 enhances anti-myeloma activity of bortezomib/proteasome inhibitor PS-341, Oncogene 23 (2004) 3597–3602.
[6] G. Teoh, M. Urashima, A. Ogata, D. Chauhan, J.A. DeCaprio, S.P. Treon, R.L. Schlossman, K.C. Anderson, MDM2 protein overexpression promotes proliferation and survival of multiple myeloma cells, Blood 90 (1997) 1982–1992.
[7] Q. Chen, W. Xie, D.J. Kuhn, P.M. Voorhees, A. Lopez-Girona, D. Mendy, L.G. Corral, V.P. Krenitsky, W. Xu, L. Moutouh-de Parseval, D.R. Webb, F. Mercurio, K.I. Nakayama, K. Nakayama, R.Z. Orlowski, Targeting the p27 E3 ligase SCF(Skp2) results in p27- and Skp2-mediated cell-cycle arrest and activation of autophagy, Blood 111 (2008) 4690–4699.
[8] M. Schwickart, X. Huang, J.R. Lill, J. Liu, R. Ferrando, D.M. French, H. Maecker, K. O'Rourke, F. Bazan, J. Eastham-Anderson, P. Yue, D. Dornan, D.C. Huang, V.M. Dixit, Deubiquitinase USP9X stabilizes MCL1 and promotes tumour cell survival, Nature 463 (2010) 103–107.
[9] N.P. Dantuma, K. Lindsten, R. Glas, M. Jellne, M.G. Masucci, Short-lived green fluorescent proteins for quantifying ubiquitin/proteasome-dependent proteolysis in living cells, Nat. Biotechnol. 18 (2000) 538–543.
[10] I. Vandenberghe, L. Creancier, S. Vispe, J.P. Annereau, J.M. Barret, I. Pouny, A. Samson, Y. Aussagues, G. Massiot, F. Ausseil, C. Bailly, A. Kruczynski, Physalin B, a novel inhibitor of the ubiquitin–proteasome pathway, triggers NOXA-associated apoptosis, Biochem. Pharmacol. 76 (2008) 453–462.
[11] V. Menendez-Benito, L.G. Verhoef, M.G. Masucci, N.P. Dantuma, Endoplasmic reticulum stress compromises the ubiquitin–proteasome system, Hum. Mol. Genet. 14 (2005) 2787–2799.
[12] S. Kharbanda, P. Pandey, L. Schofield, S. Israels, R. Roncinske, K. Yoshida, A. Bharti, Z.M. Yuan, S. Saxena, R. Weichselbaum, C. Nalin, D. Kufe, Role for Bcl-xL as an inhibitor of cytosolic cytochrome C accumulation in DNA damage-induced apoptosis, Proc. Natl. Acad. Sci. U. S. A. 94 (1997) 6939–6942.
[13] U. Hassiepen, U. Eidhoff, G. Meder, J.F. Bulber, A. Hein, U. Bodendorf, E. Lorthiois, B. Martoglio, A sensitive fluorescence intensity assay for deubiquitinating proteases using ubiquitin-rhodamine110-glycine as substrate, Anal. Biochem. 371 (2007) 201–207.
[14] V. Kapuria, L.F. Peterson, D. Fang, W.G. Bornmann, M. Talpaz, N.J. Donato, Deubiquitinase inhibition by small-molecule WP1130 triggers aggresome formation and tumor cell apoptosis, Cancer Res. 70 (2010) 9265–9276.
[15] F. Bersani, R. Taulli, P. Accornero, A. Morotti, S. Miretti, T. Crepaldi, C. Ponzetto, Bortezomib-mediated proteasome inhibition as a potential strategy for the treatment of rhabdomyosarcoma, Eur. J. Cancer 44 (2008) 876–884.
[16] A. Borodovsky, H. Ovaa, N. Kolli, T. Gan-Erdene, K.D. Wilkinson, H.L. Ploegh, B.M. Kessler, Chemistry-based functional proteomics reveals novel members of the deubiquitinating enzyme, Chem. Biol. 9 (2002) 1149–1159.
[17] K.R. Love, A. Catic, C. Schlieker, H.L. Ploegh, Mechanisms, biology and inhibitors of deubiquitinating enzymes, Nat. Chem. Biol. 3 (2007) 697–705.
[18] H. Ovaa, B.M. Kessler, U. Rolen, P.J. Galardy, H.L. Ploegh, M.G. Masucci, Activity-based ubiquitin-specific protease (USP) profiling of virus-infected and malignant human cells, Proc. Natl. Acad. Sci. U. S. A. 101 (2004) 2253–2258.
[19] M.R. Mattern, J. Wu, B. Nicholson, Ubiquitin-based anticancer therapy: carpet bombing with proteasome inhibitors vs surgical strikes with E1, E2, E3, or DUB inhibitors, Biochim. Biophys. Acta 1823 (2012) 2014–2021.
[20] G.A. Bartholomeusz, M. Talpaz, V. Kapuria, L.Y. Kong, S. Wang, Z. Estrov, W. Priebe, J. Wu, N.J. Donato, Activation of a novel Bcr/Abl destruction pathway by WP1130 induces apoptosis of chronic myelogenous leukemia cells, Blood 109 (2007) 3470–3478.
[21] K. Sukhdeo, M. Mani, T. Hideshima, K. Takada, V. Pena-Cruz, G. Mendez, S. Ito, K.C. Anderson, D.R. Carrasco, beta-catenin is dynamically stored and cleared in multiple myeloma by the proteasome–aggresome–autophagosome–lysosome pathway, Leukemia 26 (2012) 1116–1119.
[22] T. Reiner, R. Parrondo, A. de Las Pozas, D. Palenzuela, C. Perez-Stable, Betulinic acid selectively increases protein degradation and enhances prostate cancer-specific apoptosis: possible role for inhibition of deubiquitinase activity, PLoS One 8 (2013) e56234.
[23] C. Reverdy, S. Conrath, R. Lopez, C. Planquette, C. Atmanene, V. Collura, J. Harpon, V. Battaglia, V. Vivat, W. Sippl, F. Colland, Discovery of specific inhibitors of human USP7/HAUSP deubiquitinating enzyme, Chem. Biol. 19 (2012) 467–477.
[24] P. D'Arcy, S. Brnjic, M.H. Olofsson, M. Fryknas, K. Lindsten, M. De Cesare, P. Perego, B. Sadeghi, M. Hassan, R. Larsson, S. Linder, Inhibition of proteasome deubiquitinating activity as a new cancer therapy, Nat. Med. 17 (2011) 1636–1640.
[25] F. Kriegenburg, E.G. Poulsen, A. Koch, E. Kruger, R. Hartmann-Petersen, Redox control of the ubiquitin–proteasome system: from molecular mechanisms to functional significance, Antioxid. Redox Signal. 15 (2011) 2265–2299.
[26] P. Cohen, M. Tcherpakov, Will the ubiquitin system furnish as many drug targets as protein kinases? Cell 143 (2010) 686–693.
[27] M.J. Edelmann, B. Nicholson, B.M. Kessler, Pharmacological targets in the ubiquitin system offer new ways of treating cancer, neurodegenerative disorders and infectious diseases, Expert Rev. Mol. Med. 13 (2011) e35.
[28] J.E. Mullally, P.J. Moos, K. Edes, F.A. Fitzpatrick, Cyclopentenone prostaglandins of the J series inhibit the ubiquitin isopeptidase activity of the proteasome pathway, J. Biol. Chem. 276 (2001) 30366–30373.
[29] S.M. Verbitski, J.E. Mullally, F.A. Fitzpatrick, C.M. Ireland, Punaglandins, chlorinated prostaglandins, function as potent Michael receptors to inhibit ubiquitin isopeptidase activity, J. Med. Chem. 47 (2004) 2062–2070.
[30] L.M. Koharudin, H. Liu, R. Di Maio, R.B. Kodali, S.H. Graham, A.M. Gronenborn, Cyclopentenone prostaglandin-induced unfolding and aggregation of the Parkinson disease-associated UCH-L1, Proc. Natl. Acad. Sci. U. S. A. 107 (2010) 6835–6840.
[31] M. Halasi, M. Wang, T.S. Chavan, V. Gaponenko, N. Hay, A.L. Gartel, ROS inhibitor N-acetyl-L-cysteine antagonizes the activity of proteasome inhibitors, Biochem. J. 454 (2013) 201–208.
[32] D. Komander, Mechanism, specificity and structure of the deubiquitinases, Subcell. Biochem. 54 (2010) 69–87.
[33] X.M. Cotto-Rios, M. Bekes, J. Chapman, B. Ueberheide, T.T. Huang, Deubiquitinases as a signaling target of oxidative stress, Cell Rep. 2 (2012) 1475–1484.
[34] J.G. Lee, K. Baek, N. Soetandyo, Y. Ye, Reversible inactivation of deubiquitinases by reactive oxygen species in vitro and in cells, Nat. Commun. 4 (2013) 1568.
[35] Y. Kulathu, F.J. Garcia, T.E. Mevissen, M. Busch, N. Arnaudo, K.S. Carroll, D. Barford, D. Komander, Regulation of A20 and other OTU deubiquitinases by reversible oxidation, Nat. Commun. 4 (2013) 1569.
[36] F. Shang, A. Taylor, Ubiquitin–proteasome pathway and cellular responses to oxidative stress, Free Radic. Biol. Med. 51 (2011) 5–16.
[37] O.A. Issaenko, A.Y. Amerik, Chalcone-based small-molecule inhibitors attenuate malignant phenotype via targeting deubiquitinating enzymes, Cell Cycle 11 (2012) 1804–1817.
[38] M.J. Clague, Biochemistry: oxidation controls the DUB step, Nature 497 (2013) 49–50.
[39] A.F. Kabore, J. Sun, X. Hu, K. McCrea, J.B. Johnston, S.B. Gibson, The TRAIL apoptotic pathway mediates proteasome inhibitor induced apoptosis in primary chronic lymphocytic leukemia cells, Apoptosis 11 (2006) 1175–1193.
[40] H.Q. Wang, B.Q. Liu, Y.Y. Gao, X. Meng, Y. Guan, H.Y. Zhang, Z.X. Du, Inhibition of the JNK signalling pathway enhances proteasome inhibitor-induced apoptosis of kidney cancer cells by suppression of BAG3 expression, Br. J. Pharmacol. 158 (2009) 1405–1412.
[41] N. Mitsiades, C.S. Mitsiades, V. Poulaki, D. Chauhan, G. Fanourakis, X. Gu, C. Bailey, M. Joseph, T.A. Libermann, S.P. Treon, N.C. Munshi, P.G. Richardson, T. Hideshima, K.C. Anderson, Molecular sequelae of proteasome inhibition in human multiple myeloma cells, Proc. Natl. Acad. Sci. U. S. A. 99 (2002) 14374–14379.
[42] G. Hutter, Y. Zimmermann, M. Rieken, E. Hartmann, A. Rosenwald, W. Hiddemann, M. Dreyling, Proteasome inhibition leads to dephosphorylation and downregulation

of protein expression of members of the Akt/mTOR pathway in MCL, Leukemia 26 (2012) 2442–2444.
[43] D. Chauhan, Z. Tian, B. Nicholson, K.G. Kumar, B. Zhou, R. Carrasco, J.L. McDermott, C.A. Leach, M. Fulcinniti, M.P. Kodrasov, J. Weinstock, W.D. Kingsbury, T. Hideshima, P.K. Shah, S. Minvielle, M. Altun, B.M. Kessler, R. Orlowski, P. Richardson, N. Munshi, K.C. Anderson, A small molecule inhibitor of ubiquitin-specific protease-7 induces apoptosis in multiple myeloma cells and overcomes bortezomib resistance, Cancer Cell 22 (2012) 345–358.
[44] H. Sun, V. Kapuria, L.F. Peterson, D. Fang, W.G. Bornmann, G. Bartholomeusz, M. Talpaz, N.J. Donato, Bcr-Abl ubiquitination and Usp9x inhibition block kinase signaling and promote CML cell apoptosis, Blood 117 (2011) 3151–3162.
[45] A.A. Argyriou, G. Iconomou, H.P. Kalofonos, Bortezomib-induced peripheral neuropathy in multiple myeloma: a comprehensive review of the literature, Blood 112 (2008) 1593–1599.
[46] O.O. Aiyelaagbe, A.A. Hamid, E. Fattorusso, O. Taglialatela-Scafati, H.C. Schroder, W.E. Muller, Cytotoxic activity of crude extracts as well as of pure components from *Jatropha* species, plants used extensively in African traditional medicine, Evid. Based Complement. Altern. Med. 2011 (2011) 134954.
[47] S. Muangman, M. Thippornwong, R. Tohtong, Anti-metastatic effects of curcusone B, a diterpene from *Jatropha curcas*, In Vivo 19 (2005) 265–268.